

Beamforming Design for Simultaneous Transmission and Reflection Reconfigurable Intelligent Surface Assisted Secure Wireless Communication by considering Imperfect CSI

Sevedeh Reyhane Shahcheragh (1)



Department of Electrical Engineering K.N. Toosi University of Technology Tehran, Iran r.shahcheragh@email.kntu.ac.ir

Kamal Mohamed-Pour* (D)



Department of Electrical Engineering K.N. Toosi University of Technology Tehran, Iran kmpour@kntu.ac.ir

Received: 12 September 2024 - Revised: 3 August 2024 - Accepted: 22 December 2024

Abstract—This paper investigates beamforming design for Simultaneous transmission and reflection reconfigurable intelligent surface (Star RIS) assisted secure wireless communication with three operating protocols (energy splitting (ES), mode switching (MS), and time switching (TS)) with the assumption of the availability of imperfect CSI of two eavesdroppers at BS. We maximize the sum rate of legitimate users by designing both active and passive beamforming at BS and RIS, respectively, under the constraint of the limited maximum tolerable rate of eavesdroppers and a limited transmission power budget. The non-convex problem is solved by alternating optimization (AO) for active and passive beamforming optimization, and also successive convex approximation (SCA), and the penalty concave-convex procedure (PCCP). According to the simulation results, Star-RIS outperforms conventional RIS, ES mode outperforms MS and TS, and the performance is higher with lower channel estimation error.

Article type: Research Article



© The Author(s).

Publisher: ICT Research Institute

I. Introduction

In recent years, reconfigurable intelligent surface (RIS) is a potential approach to create dynamic and adaptable wireless radio propagation [1, 2]. The structure of RIS consists of numerous passive elements that are smaller than the wavelength of the signal [2, 3]. Each passive element on RIS can dynamically adjust the amplitude and phase shift of the radiated signal to RIS, which leads to deployment of smart wireless environments, so it can improve achievable data rate, remove interference, or reduce the rate of an eavesdropper [3]. Recently, to achieve full space coverage, a new type of RIS named Star-RIS has been announced, which can reflect signal in front of RIS and transmit signal behind the RIS simultaneously. This leads to the improvement of system design flexibility [4, 5]. The author in [6], studied beamforming design for Star-RIS assisted MU-MISO system to minimize the total transmit power of the BS subject to the

^{*} Corresponding Author

constraint of providing minimum user's SINR under the assumption of perfect CSI availability at the transmitter based on ES mode with equal transmission and reflection phase of each Star-RIS's element. However, the security of wireless networks is a significant aspect. RIS can improve the rate of legal users and reduce the leakage of information to eavesdroppers by adjusting wireless channels [4, 5]. As a result of the above discussions and different from [6], which minimizes BS power transmission based on assuming the availability of perfect CSI at the transmitter, we investigated secrecy communication based on assuming that the imperfect CSI of eavesdroppers is available at the transmitter due to eavesdroppers' attempt to hide their existence from BS [^{\forall]}. We maximize the sum rate of legal users subject to the constraint of limiting the wiretap rate of eavesdroppers and the constraint of limited power budget by optimizing joint BS active beamforming and Star RIS passive beamforming. The non-convex proposed problem is solved by using AO and PCCP. It should be noted that [6] solve the problem based on ES with equal transmission and reflection phase of each Star-RIS element, while we solve the problem with independent transmission and reflection phase, which leads to more degrees of freedom.

SYSTEM MODEL

Fig.1 depicts the studied system model, which includes an N antenna transmitter, two legitimate receivers, and two eavesdroppers that have singleantenna and one M-element Star RIS. Star RIS has created two distinct regions in the space surrounding itself named R region and T region. In the first region, RIS reflects the signal to the same space as the incident signal, and T region is where the RIS transmits the signal on the opposite side of the transmitter. This means that RIS transmits and reflects signals simultaneously in T and R regions, respectively. So, Star RIS has two operation modes named reflection and transmission. The receiver and eavesdropper present in region i commonly are known as receiver i, and eavesdropper i, where $i \in \{t,r\}$. Due to the existence of severe blockage, we consider the direct channels from BS and eavesdroppers and legitimate receivers to be negligible, so signals reach receivers and eavesdroppers only with the help of RIS. m-th element transmits $s_m^t = \sqrt{\beta_m^t} e^{j\theta_m^t} s_m$ and reflects $s_m^r = \sqrt{\beta_m^r} e^{j\theta_m^r} s_m$, where

 $\mathbf{S}_{\mathbf{m}}$ denotes the signal incident on the m-th element. The amplitude and phase shift of the m-th element of RIS are $\sqrt{\beta_{\rm m}^{\rm r}}, \sqrt{\beta_{\rm m}^{\rm t}} \in [0,1]$ and $\theta_{\rm m}^{\rm r}, \theta_{\rm m}^{\rm t} \in [0,2\pi)$. $\theta_{\rm m}^{\rm r}$ and $\theta_{\rm m}^{\rm t}$ operate independently of each other, but the conservation of energy principle leads to dependent amplitude on T and R region, i.e., the total energy of radiated signal on an element should be equal to the sum of signal's energies at region T and region R, which means $\left|s_m^t\right|^2 + \left|s_m^r\right|^2 = \left|s_m\right|^2$ and $\beta_m^t + \beta_m^r = 1$ where,

means
$$|s_m^t|^2 + |s_m^r|^2 = |s_m|^2$$
 and $\beta_m^t + \beta_m^t = 1$ where, $m \in M \square \{1, 2, ..., M\} [8].$

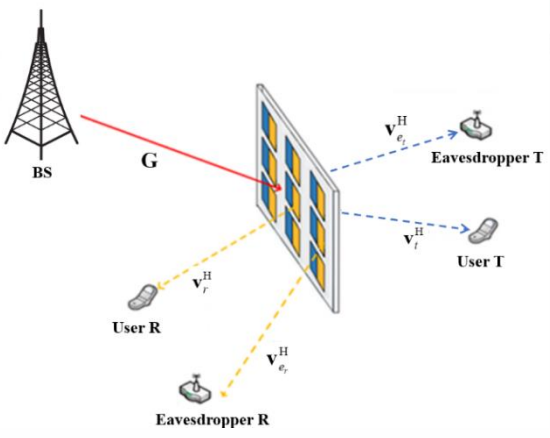


Figure 1. System Model

Based on the above discussion, three operating protocols of Star-RIS i.e. ES, MS, and TS are explained below.

In ES, the incident signal's energy on each element is separated into two parts for signal reflection in the R region and signal transmission in the T region proportional to $\beta_m^r : \beta_m^t$. ES has the highest DoFs in practical protocols due to enabling simultaneous design of both Star-RIS coefficients, which are expressed as

$$\mathbf{\Phi}_{r}^{ES} = \operatorname{diag}(\sqrt{\beta_{1}^{r}} e^{j\theta_{1}^{r}}, \sqrt{\beta_{2}^{r}} e^{j\theta_{2}^{r}}, ..., \sqrt{\beta_{M}^{r}} e^{j\theta_{M}^{r}}), \qquad (1)$$

$$\begin{split} & \boldsymbol{\Phi}_{t}^{ES} = diag(\sqrt{\beta_{1}^{t}} e^{j\theta_{1}^{t}}, \sqrt{\beta_{2}^{t}} e^{j\theta_{2}^{t}}, ..., \sqrt{\beta_{M}^{t}} e^{j\theta_{M}^{t}}), \end{aligned} \tag{2} \\ & \text{where } \boldsymbol{\theta}_{m}^{r}, \boldsymbol{\theta}_{m}^{t} \in [0, 2\pi) \text{ , } \sqrt{\beta_{m}^{r}}, \sqrt{\beta_{m}^{t}} \in [0, 1] \text{ , } \boldsymbol{\beta}_{m}^{r} + \boldsymbol{\beta}_{m}^{t} = 1 \text{ , } \\ & m \in M \square \left\{1, 2, ..., M\right\} \left[8\right]. \end{split}$$

In MS, all Star RIS elements are divided into two parts, M_r elements and M_r elements, which work in transmission and reflection modes, respectively. MS is classified as a unique instance of ES due to binary coefficients. Thus, the degree of freedom is reduced, and the performance may be degraded compared to ES. According to the above explanation, the Star-RIS coefficients are expressed as

$$\mathbf{\Phi}_{r}^{MS} = diag(\sqrt{\beta_{l}^{r}} e^{j\theta_{l}^{r}}, \sqrt{\beta_{2}^{r}} e^{j\theta_{2}^{r}}, ..., \sqrt{\beta_{M}^{r}} e^{j\theta_{M}^{r}})$$
 (3)

$$\begin{split} & \boldsymbol{\Phi}_{t}^{MS} = diag(\sqrt{\beta_{1}^{t}}e^{j\theta_{1}^{t}},\sqrt{\beta_{2}^{t}}e^{j\theta_{2}^{t}},...,\sqrt{\beta_{M}^{t}}e^{j\theta_{M}^{t}}), \\ & \text{where } \boldsymbol{\theta}_{m}^{r},\boldsymbol{\theta}_{m}^{t} \in [0,2\pi) \text{ , } \sqrt{\beta_{m}^{r}},\sqrt{\beta_{m}^{t}} \in \{0,1\} \text{ , } \boldsymbol{\beta}_{m}^{r}+\boldsymbol{\beta}_{m}^{t}=1 \text{ ,} \\ & \text{where } m \in M \; \square \; \{1,2,...,M\} \; [8]. \end{split}$$

In TS mode, there is a time allocation for reflection and transmission mode. In other words, all elements are in reflection or transmission mode in orthogonal time slots. Let $\tau_i \in [0,1]$ be the time allocation that satisfies $\tau_t + \tau_r = 1$. Unlike energy splitting and mode switching, the coefficients are independent in time switching mode, but precise time synchronization is needed. In this protocol, the Star-RIS coefficients are as below

$$\Phi_{r}^{TS} = diag(e^{j\theta_{r}^{f}}, e^{j\theta_{2}^{f}}, ..., e^{j\theta_{M}^{f}}),$$
(5)

$$\mathbf{\Phi}_{t}^{TS} = \operatorname{diag}(e^{j\theta_{t}^{l}}, e^{j\theta_{2}^{l}}, ..., e^{j\theta_{M}^{l}}), \tag{6}$$

where $\theta_m^r, \theta_m^t \in [0, 2\pi)$ and $m \in M \square \{1, 2, ..., M\} \lceil \Lambda \rceil$.

We suppose that direct communication between transmitter and receivers and between transmitter and eavesdropper is impossible due to server blockage between them. Rayleigh flat fading channels $\mathbf{V}_i^H \in \square^{\ l \times M} \ , \ \mathbf{V}_{e,i}^H \in \square^{\ l \times M} \ \text{and} \ \mathbf{G} \in \square^{\ M \times N} \ \text{which are given below, denote the channel from Star RIS to user i and eavesdropper i, BS to Star RIS, respectively}$

$$\mathbf{G} = \sqrt{\frac{\rho_0}{\mathbf{d}_{BR}^{\alpha}}} \mathbf{G}^{\text{NLOS}} \tag{7}$$

$$\mathbf{v}_{j} = \sqrt{\frac{\rho_{0}}{d_{Ru}^{\alpha_{j}}}} \mathbf{v}_{j}^{NLOS}, j \in \mathbf{J} = \{\mathbf{r}, \mathbf{t}, \mathbf{e}_{r}, \mathbf{e}_{t}\}, \tag{8}$$

The pass loss at 1 meter distance is denoted by ρ_0 . d_{BR} and d_{Ru} indicate the distance from the transmitter to RIS and from RIS to j-th node. $\alpha_j \geq 2$ is the path loss exponent. Rayleigh fading is used to model the nonline-of-sight components, represented by $\mathbf{G}^{\text{NLOS}} \in \square^{\text{M} \times \text{N}}$ and $\mathbf{V}_j^{\text{NLOS}} \in \square^{\text{M} \times \text{I}}$ where $j \in J = \{r, t, e_r, e_t\}$.

In this system, the base station concurrently transmits signals $s_i \sim CN(0,1)$ with beamforming vector $\mathbf{w}_i \in \mathbb{D}^{N\times 1}$ to legitimate users located in region i while eavesdropper i attempts to eavesdrop the information of user i, where $i \in \{t,r\}$. RIS conveys transmitted information from BS to receivers. The received signals by legitimate users and eavesdroppers are expressed as

$$\mathbf{y}_{i} = \mathbf{v}_{i}^{H} \mathbf{\Phi}_{i}^{H} \mathbf{G} \left(\sum_{j=r,t} \mathbf{w}_{j} \mathbf{s}_{j} \right) + \mathbf{n}_{i}, \tag{9}$$

$$y_{e,i} = \mathbf{v}_{e,i}^{H} \mathbf{\Phi}_{i}^{H} \mathbf{G}(\sum_{j=r,t} \mathbf{w}_{j} s_{j}) + n_{e,i}.$$
 (10)

 n_i and $n_{e,i}$ are additive white Gaussian noises (AWGN) with a mean of zero and variance of σ_i^2 and σ_e^2 . BS computes Star-RIS coefficients and feeds them back to the RIS controller via dedicated feedback channels. The diagonal element of Φ_i is denoted as $\theta_i = \text{diag}(\Phi_i) \in \square^{M\times l}$ [9], and the equivalent channels from BS to legitimate users and eavesdroppers are represented below

$$\mathbf{H}_{i} = \operatorname{Diag}(\mathbf{v}_{i}^{H})\mathbf{G}, \forall j \in \{r, t, e_{r}, e_{t}\}, \tag{11}$$

So, based on the above equivalent channels, users and eavesdroppers receive signals written below.

$$\mathbf{y}_{i} = \boldsymbol{\theta}_{i}^{H} \mathbf{H}_{i} \left(\sum_{j=r,t} \mathbf{w}_{j} s_{j} \right) + \mathbf{n}_{i}, \tag{12}$$

$$\mathbf{y}_{e,i} = \boldsymbol{\theta}_{i}^{H} \mathbf{H}_{e_{i}} \left(\sum_{j=r,t} \mathbf{w}_{j} \mathbf{s}_{j} \right) + \mathbf{n}_{e,i}.$$
 (13)

The data rate at user i is expressed as

$$R_{u,i} = log(1 + \frac{\left|\boldsymbol{\theta}_{i}^{H} \mathbf{H}_{i} \mathbf{w}_{i}\right|^{2}}{\left|\boldsymbol{\theta}_{i}^{H} \mathbf{H}_{i} \mathbf{w}_{i'}\right|^{2} + \sigma_{u,i}^{2}}).$$
(14)

We assume that Eve i exclusively wiretap the transmitted information for user i, so the data rate at i-th Eve is expressed as

$$R_{e,i} = log(1 + \frac{\left|\boldsymbol{\theta}_{i}^{H} \mathbf{H}_{e_{i}} \mathbf{w}_{i}\right|^{2}}{\left|\boldsymbol{\theta}_{i}^{H} \mathbf{H}_{e_{i}} \mathbf{w}_{i}\right|^{2} + \sigma_{e,i}^{2}}). \tag{15}$$

We assume that BS has constrained power available for transmitting signals as below.

$$\sum_{i=r,t} \left\| \mathbf{w}_i \right\|_2^2 \le P_{\text{max}} \tag{16}$$

III. PROBLEM FORMULATION

It is assumed that perfect CSI for the link between BS and legitimate users through RIS is available due to cooperation between legitimate users and BS for CSI acquisition. However, the potential eavesdroppers don't assist the transmitter in acquiring channel state information and interact with the dedicated system less frequently to hide their existence from the transmitter. So, by utilizing signal leakage from these potential eavesdroppers, BS obtains outdated or imperfect CSI due to feedback delay and untrustworthy feedback information [7]. So, we assume that just imperfect CSI for cascade channel form BS to eavesdropper *i* is available, and the error is modeled by bounded CSI error as below.

$$\mathbf{H}_{\mathrm{e,i}} = \mathbf{H}_{\mathrm{e,i}} + \Delta \mathbf{H}_{\mathrm{e,i}}, \tag{17}$$

$$\Omega = \{ \Delta \mathbf{H}_{e,i} \in \Box^{M \times N} : \| \Delta \mathbf{H}_{e,i} \| \le \varepsilon \}, \tag{18}$$

where $\mathbf{H}_{\mathrm{e,i}}$ denotes the estimated channel of i-th eavesdropper's, $\Delta\mathbf{H}_{\mathrm{e,i}}$ denotes error of i-th eavesdropper's estimated CSI, and ε denotes radii of CSI uncertainty range known at the BS [9]. Ω represents a continuous set that encompasses all CSI estimation errors with norms bounded by $\varepsilon > 0$ [7].

$$\max_{\mathbf{w}_{i}, \theta_{i}} \sum_{i=-1}^{n} \mathbf{R}_{u,i} \tag{19a}$$

subject to:
$$\max_{\Delta \mathbf{H}_{e,i} \in \Omega} R_{e,i} \leq R_{M}$$
, (19b)

$$\sum_{i=r} \left\| \mathbf{w}_i \right\|^2 \le P_T, \tag{19c}$$

$$\sum_{i=r,t} diag(\boldsymbol{\theta}_i \boldsymbol{\theta}_i^{H}) = \boldsymbol{1}_{l \times M}, \qquad (19d)$$

where R_M is the maximum rate of eavesdropper i for obtaining the information of user i in (19d),

constraint (19c) indicates the total transmission power budget $\,P_{\rm T}$, and (19d) denotes the ES coefficient constraint.

The optimization issue in equation (19) lacks convexity due to the non-concave nature of the objective function (19a), the presence of infinite non-convex constraints in (19b), and the constraint related to the ES coefficient of Star-RIS (19d).

We solve the problem (19) by implementing an AO algorithm to optimize active and passive beamforming in an alternating manner. We also implement the SCA approach to convert each subproblem into a series of approximated convex problems, each one can be individually solved with the help of conventional optimization tools like CVX. Moreover, we convert the non-convex problem to convex one with the help of S-Procedure, pass following method, and PCCP.

First, we reformulate the objective function (19a) using the path following lemma.

Lemma1: Path following method around the given points, $\{\tilde{u}, \tilde{v}\}[8]$ holds inequality (20):

$$\ln\left(1 + \frac{\left|u\right|^{2}}{v}\right) \ge \ln\left(1 + \frac{\left|\tilde{u}\right|^{2}}{v}\right) - \frac{\left|\tilde{u}\right|^{2}}{\tilde{v}} + \frac{2\Re\{u\tilde{u}\}}{\tilde{v}} - \frac{\left|\tilde{u}\right|^{2}\left(v + u^{2}\right)}{\tilde{v}(\tilde{v} + \tilde{u}^{2})}, \tag{20}$$

Hence, around fixed points, we have

$$\begin{split} R_{u,i} &\geq \log(1 + c_{li} \left| \tilde{\boldsymbol{\theta}}_{i}^{H} \boldsymbol{H}_{i} \tilde{\boldsymbol{w}}_{i} \right|^{2}) - c_{li} \left| \tilde{\boldsymbol{\theta}}_{i}^{H} \boldsymbol{H}_{i} \tilde{\boldsymbol{w}}_{i} \right|^{2} \\ &+ c_{li} 2 \Re \{ \boldsymbol{w}_{i}^{H} \boldsymbol{H}_{i}^{H} \boldsymbol{\theta}_{i} \tilde{\boldsymbol{\theta}}_{i}^{H} \boldsymbol{H}_{i} \tilde{\boldsymbol{w}}_{i} \} \\ &- c_{2i} (\left| \boldsymbol{\theta}_{i}^{H} \boldsymbol{H}_{i} \boldsymbol{w}_{i} \right|^{2} + \left| \boldsymbol{\theta}_{i}^{H} \boldsymbol{H}_{i} \boldsymbol{w}_{i'} \right|^{2} + \sigma_{i}^{2}) , \end{split}$$

$$(21)$$

$$\mathbf{c}_{li} = \frac{1}{\left|\tilde{\boldsymbol{\theta}}_{i}^{H} \mathbf{H}_{i} \tilde{\mathbf{w}}_{i}\right|^{2} + \sigma_{i}^{2}},$$
(22)

$$c_{2i} = \frac{c_{1i} \left| \tilde{\boldsymbol{\theta}}_{i}^{H} \mathbf{H}_{i} \tilde{\mathbf{w}}_{i} \right|^{2}}{\left| \tilde{\boldsymbol{\theta}}_{i}^{H} \mathbf{H}_{i} \tilde{\mathbf{w}}_{i} \right|^{2} + \left| \tilde{\boldsymbol{\theta}}_{i}^{H} \mathbf{H}_{i} \tilde{\mathbf{w}}_{i'} \right|^{2} + \sigma_{i}^{2}}.$$
(23)

Based on equation (21) and neglecting the constant terms, (19a) is converted to convex form w.r.t. $\mathbf{w}_{i}, \mathbf{\theta}_{i}$ [10].

Lemma 2: Based on General S-Procedure [9], quadratic functions of the variable $\mathbf{x} \in \Box^{n \times l}$ are defined so that,

$$g_{i}(\mathbf{x}) = \mathbf{x}^{H} \mathbf{W}_{i} \mathbf{x} + 2\Re{\{\mathbf{w}_{i}^{H} \mathbf{x}\}} + w_{i}, \forall i = 0,...,P,$$
 (24)

where $\mathbf{W}_i = \mathbf{W}_i^H$. If $\overline{w}_i \geq 0$ exists, then $\{g_i(x) \geq 0\}_{i=1}^P \Rightarrow g_o(x) \geq 0$ is satisfied and vice versa, such that

$$\begin{bmatrix} \mathbf{W}_0 & \mathbf{w}_0 \\ \mathbf{w}_0 & \mathbf{w}_0 \end{bmatrix} - \sum_{i=1}^{P} \overline{\mathbf{w}}_i \begin{bmatrix} \mathbf{W}_i & \mathbf{w}_i \\ \mathbf{w}_i & \mathbf{w}_i \end{bmatrix} \pm 0.$$
 (25)

Lemma 3: Based on general sign definiteness [9], the linear matrix (26) is satisfied for given $\mathbf{W} = \mathbf{W}^{H}$, $\{\mathbf{Y}_{i}, \mathbf{Z}_{i}\}_{i=1}^{P}$

$$\mathbf{W} \pm \sum_{i=1}^{P} (\mathbf{Y}_{i}^{H} \mathbf{X}_{i} \mathbf{Z}_{i} + \mathbf{Z}_{i}^{H} \mathbf{X}_{i} \mathbf{Y}_{i}), \forall i, \|\mathbf{X}_{i}\|_{F} \leq \varepsilon_{i}$$
 (26)

if and only if there exist real numbers $\lambda_i \ge 0$ such that

$$\begin{bmatrix} \mathbf{W} - \sum_{i=1}^{P} \lambda_{i} \mathbf{Z}_{i}^{H} \mathbf{Z}_{i} & -_{s_{1}} \mathbf{Y}_{1}^{H} & \dots & -_{p} \mathbf{Y}_{p}^{H} \\ -_{s_{1}} \mathbf{Y}_{1}^{\square} & \lambda_{i} \mathbf{I} & \dots & \mathbf{0} \\ -_{s_{p}} \mathbf{Y}_{p}^{\square} & \mathbf{0} & \dots & \lambda_{p} \mathbf{I} \end{bmatrix} \pm 0.$$
 (27)

By using auxiliary variables β_i , equation (19b) is equivalent to two constraints as below.

$$\left|\mathbf{\theta}_{i}^{H}\mathbf{H}_{e,i}\mathbf{w}_{i}\right|^{2} \leq \beta_{i}(2^{R_{M}}-1),\tag{28}$$

$$\left|\boldsymbol{\theta}_{i}^{H}\boldsymbol{H}_{e,i}\boldsymbol{w}_{i'}\right|^{2} \geq \beta_{i} - \sigma_{i}^{2}.$$
 (29)

The infinite linear inequalities (28), are converted into finite matrix inequalities by using Schur's complement lemma as shown below.

$$\begin{bmatrix} \beta_{i}(2^{R_{M}}-1) & \mathbf{t}_{i}^{H} \\ \vdots & \mathbf{I} \end{bmatrix} \geq 0.$$
 (30)

Where $\mathbf{t}_{i}^{H} = \mathbf{\theta}_{i}^{H} \mathbf{H}_{e,i} \mathbf{w}_{i}$. By using $\mathbf{H}_{e,i} = \mathbf{H}_{e,i} + \Delta \mathbf{H}_{e,i}$ equation (30) is then reformulated as

$$\begin{bmatrix}
\beta_{i}(2^{R_{M}}-1) & \mathbf{t}_{i}^{H} \\
\mathbf{t}_{i} & \mathbf{I}
\end{bmatrix} + \begin{bmatrix}
\mathbf{0} \\
\mathbf{w}_{i}^{H}
\end{bmatrix} \Delta \mathbf{H}_{e,i}^{H} \begin{bmatrix}
\mathbf{0} \\
\mathbf{0}
\end{bmatrix} \Delta \mathbf{H}_{e,i}^{H} \begin{bmatrix}
\mathbf{0} & \mathbf{w}_{i}
\end{bmatrix} \ge 0, \quad (31)$$

then, by using Lemma 3, the given LMIs are equivalent

to

$$\begin{bmatrix} \beta_{i}(2^{R_{M}}-1)-\mu_{i}(\mathbf{Z}\mathbf{Z}^{H}) & \mathbf{t}_{i}^{H} & \mathbf{0} \\ \mathbf{t}_{i} & \mathbf{I} & \varepsilon_{g}\mathbf{w}_{i}^{H} \\ \mathbf{0} & \varepsilon_{g}\mathbf{w}_{i} & \mu_{i}\mathbf{I} \end{bmatrix} \geq 0, \forall i = r, t,$$
(32)

where $\mathbf{Z} = \begin{bmatrix} \mathbf{\theta}_1 & \mathbf{0} \end{bmatrix}$.

Then for the non-convex semi-infinite inequalities (29), we first approximate the non-convex part, and then, by using S-Procedure we handle the semi-infinite inequalities.

Volume 17- Number 2 – 2025 (1-8)

So first, we linearly approximate the left side of constraint (29) by its lower bound as below [9]

$$\operatorname{vec}^{\mathrm{T}}(\Delta \mathbf{H}_{e,i}) \mathbf{B}_{i} \operatorname{vec}(\Delta \mathbf{H}_{e,i}^{*}) + 2\Re \{ \mathbf{b}_{i}^{\mathrm{T}}(\Delta \mathbf{H}_{e,i}^{*}) \} + \mathbf{b}_{i}$$
 (33)

where.

$$\mathbf{B}_{i} = \mathbf{w}_{i} \mathbf{w}_{i}^{(n)H} \otimes \mathbf{\theta}_{i}^{*} \mathbf{\theta}_{i}^{(n)T} + \mathbf{w}_{i}^{(n)} \mathbf{w}_{i}^{H} \otimes \mathbf{\theta}_{i}^{n*} \mathbf{\theta}_{i}^{T}$$

$$-\mathbf{w}_{i}^{(n)} \mathbf{w}_{i}^{(n)H} \otimes \mathbf{\theta}_{i}^{n*} \mathbf{\theta}_{i}^{(n)T}, \tag{34}$$

$$\boldsymbol{b}_{_{i}} = \text{vec}(\boldsymbol{\theta}_{_{i}}\boldsymbol{\theta}_{_{i}}^{(n)H}\stackrel{\bar{\boldsymbol{H}}_{e,i}}{\boldsymbol{H}_{e,i}}\stackrel{\bar{\boldsymbol{w}}_{_{i}}^{H}}{\boldsymbol{w}_{_{i}}^{H}}) + \text{vec}(\boldsymbol{\theta}_{_{i}}^{(n)}\boldsymbol{\theta}_{_{i}}^{H}\stackrel{\bar{\boldsymbol{U}}_{e,i}}{\boldsymbol{H}_{e,i}}\stackrel{\bar{\boldsymbol{w}}_{_{i}}^{(n)}\boldsymbol{w}_{_{i}}^{(n)H}}{\boldsymbol{W}_{_{i}}^{(n)H}})$$

$$-\text{vec}(\boldsymbol{\theta}_{i}^{(n)}\boldsymbol{\theta}_{i}^{(n)H} \overset{-}{\mathbf{H}}_{e,i} \mathbf{w}_{i}^{(n)}\mathbf{w}_{i}^{(n)H}), \quad (35)$$

$$b_{i} = 2\Re\{\theta_{i}^{(n)H} \stackrel{-}{\mathbf{H}} \mathbf{w}_{i}^{(n)} \mathbf{w}_{i}^{H} \stackrel{-}{\mathbf{H}}_{e,i} \theta_{i}\} - \theta_{i}^{(n)H} \stackrel{-}{\mathbf{H}}_{e,i}^{H} \mathbf{w}_{i}^{(n)} \mathbf{w}_{i}^{(n)H} \stackrel{-}{\mathbf{H}}_{e,i}^{H} \theta_{i}^{(n)},$$
(36)

Then, by using S-Procedure, slack variables $\omega_{g,i} \geq 0$ and $C_i^{\text{partial}} = b_i - \beta_i (2^{R_i} - 1) - \omega_{g,i} \varepsilon^2$, equation (29) is transformed into the following LMIs as

$$\begin{bmatrix} \omega_{g,i} \mathbf{I} + \mathbf{B}_{i} & \mathbf{b}_{i} \\ \mathbf{b}_{i}^{T} & C_{i}^{partial} \end{bmatrix} \ge 0, \tag{37}$$

Finally, problem (19), based on the above solution, is reformulated below

$$\begin{aligned} Min_{\mathbf{w}_{i},\mathbf{\theta}_{i},\mu_{i},\omega_{g,i}} & & \sum_{i=r,t} 2\Re\{\mathbf{w}_{i}^{H}\mathbf{w}_{i}\mathbf{\theta}_{i}\mathbf{\theta}_{i}^{H}\} \\ & & & -c_{2i}\left(\left|\mathbf{\theta}_{i}^{H}\mathbf{H}_{i}\mathbf{w}_{i}\right|^{2} + \left|\mathbf{\theta}_{i}^{H}\mathbf{H}_{i}\mathbf{w}_{i'}\right|^{2}\right) \end{aligned} \tag{38a}$$

$$\omega_{g,i}, \mu_i \ge 0, \forall i = r, t$$
 (38c)

We should point out that the problem (38) remains non-convex, and solving it is challenging due to the coupled variables. So, we utilize the AO to optimize \mathbf{w}_i and $\boldsymbol{\theta}_i$ in an alternative manner. First, we solve the convex problem with respect to \mathbf{w}_i , as shown below

$$\begin{split} \boldsymbol{w}_{i}^{(n+1)} &= arg \, min_{\boldsymbol{w}_{i},\boldsymbol{\mu}_{i},\boldsymbol{\omega}_{g,i}} & \sum_{i=r,t} 2\Re\{\boldsymbol{w}_{i}^{H}\boldsymbol{w}_{i}\boldsymbol{\theta}_{i}\boldsymbol{\theta}_{i}^{H}\} \\ & -c_{2i}(\left|\boldsymbol{\theta}_{i}^{H}\boldsymbol{H}_{i}\boldsymbol{w}_{i}\right|^{2} + \left|\boldsymbol{\theta}_{i}^{H}\boldsymbol{H}_{i}\boldsymbol{w}_{i'}\right|^{2}) \quad (39a) \end{split}$$

Then, we use new slack variables α_i to improve the convergence of the problem with respect to θ_i [9], so equation (29) is reformulated as

$$\left|\mathbf{\theta}_{i}^{H}\mathbf{H}_{e,i}\mathbf{w}_{i'}\right|^{2} \geq \beta_{i} - \sigma_{i}^{2} + \alpha_{i}, \tag{40}$$

Based on (40), the LMIs in (37) are reformulated as

$$\begin{bmatrix} \omega_{g,i} \mathbf{I} + \mathbf{B}_{i} & \mathbf{b}_{i} \\ \mathbf{b}_{i}^{T} & C_{i}^{\text{partial}} - \alpha_{i} \end{bmatrix} \ge 0, \tag{41}$$

Based on the above solutions, the sub-problem optimization with respect to θ_i is given by

$$\begin{aligned} \operatorname{Min}_{\boldsymbol{\theta}_{i},\alpha_{i},\mu_{i},w_{g,i}} & & \sum_{i=r,t} 2\Re\{\boldsymbol{w}_{i}^{H}\boldsymbol{w}_{i}\boldsymbol{\theta}_{i}\boldsymbol{\theta}_{i}^{H}\} \\ & & & -c_{2i}(\left|\boldsymbol{\theta}_{i}^{H}\boldsymbol{H}_{i}\boldsymbol{w}_{i}\right|^{2} + \left|\boldsymbol{\theta}_{i}^{H}\boldsymbol{H}_{i}\boldsymbol{w}_{i'}\right|^{2}) \end{aligned} \tag{42a}$$

$$\alpha_i \ge 0 \quad \forall i = r, t$$
 (42b)

Problem (42) remains non-convex due to (19d), which is solved by auxiliary variables $\begin{aligned} & \mathbf{x}_i = [x_{i,1},...,x_{i,M}] & \text{that } \mathbf{x}_{i,m} = [\boldsymbol{\theta}_i]_m^* [\boldsymbol{\theta}_i]_m & \text{. Then by} \\ & \text{considering} & \mathbf{x}_{i,m} \leq [\boldsymbol{\theta}_i]_m^* [\boldsymbol{\theta}_i]_m \leq \mathbf{x}_{i,m} & , & \text{and} \\ & \text{approximating} & \text{the left side of it as,} \\ & \mathbf{x}_{i,m} \leq 2\Re\{[\boldsymbol{\theta}_i]_m^* [\tilde{\boldsymbol{\theta}}_i]_m\} - [\tilde{\boldsymbol{\theta}}_i]_m^* [\tilde{\boldsymbol{\theta}}_i]_m & , & \text{and also using} \\ & \text{slack variables} & \mathbf{y}_{i,m} \geq 0 & , & \sum_{m=1}^{2M} \mathbf{y}_{i,m} & \text{is added to the} \\ & \text{objective as the penalty term [11], so the solved problem (42) is given below} \end{aligned}$

$$\begin{split} Min_{\boldsymbol{\theta}_{i},\alpha_{i},\mu_{i},\mathbf{w}_{g,i}} & & \sum_{i=r,t} 2\mathfrak{R}\{\boldsymbol{w}_{i}^{H}\boldsymbol{w}_{i}\boldsymbol{\theta}_{i}\boldsymbol{\theta}_{i}^{H}\} \\ & & -c_{2i}(\left|\boldsymbol{\theta}_{i}^{H}\boldsymbol{H}_{i}\boldsymbol{w}_{i}\right|^{2} + \left|\boldsymbol{\theta}_{i}^{H}\boldsymbol{H}_{i}\boldsymbol{w}_{i'}\right|^{2}) \\ & & + \eta^{[n]}\sum_{i}\sum_{i}^{2M}y_{i,m} \end{split} \tag{43a}$$

$$\alpha_i \ge 0$$
 (43c)

$$-2\Re\{[\boldsymbol{\theta}_{i}]_{m}^{*}[\tilde{\boldsymbol{\theta}}_{i}]_{m}\}+[\tilde{\boldsymbol{\theta}}_{i}]_{m}^{*}[\tilde{\boldsymbol{\theta}}_{i}]_{m}\leq \mathbf{y}_{i,m+M}-\mathbf{x}_{i,m} \quad (43d)$$

$$[\boldsymbol{\theta}_{i}]_{m}^{*}[\boldsymbol{\theta}_{i}]_{m} \leq \mathbf{x}_{i,m} + \mathbf{y}_{i,m} \tag{43e}$$

$$\sum_{i=r,t} \boldsymbol{x}_{i,m} = 1, \boldsymbol{x}_{i,m} \geq 0, \forall m \in M, \forall i=r,t \tag{43f} \label{eq:43f}$$

IV. INVESTIGATING MS AND TS MODE

A. Problem optimization in MS mode

In MS, with given θ_i , the optimization of \mathbf{w}_i is the same as ES. With given \mathbf{w}_i , since the altitude of coefficients is binary, the difference part from ES in optimization of θ_i is $\mathbf{x}_{i,m} \in \{0,1\}$, so we have a nonconvex mixed-integer problem. Introducing slack

variables $\mathbf{Z}_{i,m}$ allows us to deal with the non-convexity, and it is provable that $\mathbf{x}_{i,m} \in \{0,1\}$ equals to $\mathbf{x}_{i,m} = \mathbf{z}_{i,m}$ and $\mathbf{x}_{i,m} (1-\mathbf{z}_{i,m}) = 0$ [11]. Next, the penalty term (45) is added into the objective function, and in the \mathbf{n}_{th} iteration, $\boldsymbol{\rho}^n$ is a penalty factor which is refreshed in the same manner as $\boldsymbol{\eta}^n$, subsequently with given $\{\boldsymbol{\theta}_i, \mathbf{x}_i, \mathbf{y}_i\}$, the value of $\mathbf{Z}_{i,m}$ is calculated by the following formula,

$$(\mathbf{x}_{i,m} + (\mathbf{x}_{i,m})^2) / (1 + (\mathbf{x}_{i,m})^2)$$
 (44)

so, with given $\mathbf{z}_{i,m}$ in the previous iteration, the variables in PCCP method are determined [12].

$$\rho^{n} \sum_{i=r, l} \sum_{m=l}^{M} (|\mathbf{x}_{i,m} - \mathbf{z}_{i,m}|^{2} + |\mathbf{x}_{i,m}(1 - \mathbf{z}_{i,m})|^{2})$$
(45)

B. Problem optimization in TS

In TS, we introduce a two-layer optimization problem. We implement a similar method, especially for the given τ_i , so we have the following sub-problem.

$$\begin{aligned} \operatorname{Min}_{\boldsymbol{\theta}_{i},\alpha_{i},\mu_{i},\operatorname{w}_{g,i}} & & \sum_{i=r,t} \tau_{i} [2\mathfrak{R}\{\boldsymbol{w}_{i}^{H}\boldsymbol{w}_{i}\boldsymbol{\theta}_{i}\boldsymbol{\theta}_{i}^{H}\} \\ & & -c_{2i}(\left|\boldsymbol{\theta}_{i}^{H}\boldsymbol{H}_{i}\boldsymbol{w}_{i}\right|^{2})] \end{aligned} \tag{46a}$$

subject to:
$$(32)$$
, (37) , $(19c)$, $\mu_i \ge 0$ (46b)

$$[\theta_{i}]_{m} = e^{j\varphi_{m}^{i}}, \varphi_{m}^{i} \in [0, 2\pi), \forall m \in M$$
 (46c)

$$\tau_{i} \in [0,1], \sum_{i} \tau_{i} = 1,$$
 (46d)

where,

$$c_{li} = \frac{1}{\sigma_i^2}, \tag{47}$$

$$c_{2i} = \frac{c_{1i} \left| \tilde{\boldsymbol{\theta}}_{i}^{H} \mathbf{H}_{i} \tilde{\mathbf{w}}_{i} \right|^{2}}{\left| \tilde{\boldsymbol{\theta}}_{i}^{H} \mathbf{H}_{i} \tilde{\mathbf{w}}_{i} \right|^{2} + \sigma_{i}^{2}}.$$
(48)

Since TS is interference-free, it can be more straightforward than other protocols. After solving (46), which optimizes \mathbf{w}_i and $\mathbf{\theta}_i$ with given τ_i , we calculate the optimal value of τ_i by exhaustive search [13].

V. CONVERGENCE ANALYSIS

The detail of the convergence behavior of the proposed algorithm is determined as follows. Since \mathbf{w}_i and $\mathbf{\theta}_i$ are optimized iteratively by implementing an alternating approach, let $R_{sum}(\mathbf{w}_i^k, \mathbf{\theta}_i^k)$ denotes the objective value of (19) in the $\mathbf{k}_{_}$ th iteration. Let $R_{sum}(\mathbf{w}_i^{k+1}, \mathbf{\theta}_i^k)$ and $R_{sum}(\mathbf{w}_i^{k+1}, \mathbf{\theta}_i^{k+1})$ be the objective function of problems (39) and (43), respectively. Then we have inequality (49):

$$R_{sum}(\mathbf{w}_{i}^{k}, \mathbf{\theta}_{i}^{k}) \leq R_{sum}(\mathbf{w}_{i}^{k+1}, \mathbf{\theta}_{i}^{k}) \leq R_{sum}(\mathbf{w}_{i}^{k+1}, \mathbf{\theta}_{i}^{k+1}).$$
 (49) The inequality in (49) denotes that after each iteration the objective function (19) is monotonically non-decreasing [14] and since \mathbf{w}_{i} and $\mathbf{\theta}_{i}$ are bounded by (19c) and (19d), respectively, $R_{sum}(\mathbf{w}_{i}^{k}, \mathbf{\theta}_{i}^{k})$ is converged to a limit optimal point $R_{sum}(\mathbf{w}^{opt}, \mathbf{\theta}^{opt})$ [15].

VI. SIMULATION RESULTS

In this section, we demonstrate the numerical results to evaluate the effectiveness of our proposed scenario. We assume that users are positioned at a circle with a radius of 5 meters, and eavesdroppers at a circle with a radius of 10 meters which are centered at the RIS. Some detailed parameters are illustrated in Table 1. In our results, we compare the performance of three operating protocols of M elements Star-RIS, which are ES, MS, and TS, with M elements conventional RIS, which is the combination of one reflection RIS and transmission RIS with M/2 elements. Fig.2, shows sum secrecy rate of legitimate users versus the effect of increasing the transmit power. Moreover, we show the impact of different channel uncertainties in this figure. Star-RIS outperforms conventional RIS in terms of performance to reflecting and transmitting signals simultaneously, while conventional RIS reflects signals, which leads to more DoFs for Star-RIS than conventional RIS. Moreover, in Star-RIS, when the transmit power is relatively small, TS is superior to ES and MS due to interference-free communications in TS. But with relatively large transmit power, the performance of ES and MS outperform TS since the interference in ES and MS restricts the wiretap rate of eavesdroppers when optimized properly, and in the TS both legal user rate and wiretap rate increase with more transmit power. Thus, the SSR is restricted with more transmit power in TS. Also, between ES and MS, ES outperforms MS since ES has continuous altitude coefficients in contrast to binary altitude coefficients of MS which is a special case of ES with fewer DoFs. Moreover, we compare the results for different channel uncertainty, i.e., $\varepsilon = 0.001$ $\varepsilon = 0.01$. The performance reduces with higher channel uncertainty in all methods due to more difficult precise beamforming, and higher channel uncertainty leads to the use of some transmission power for compensating channel estimation error.

TABLE I. SIMULATION PARAMETERS

Parameter	Value
Path loss exponents	$\alpha = 2.2$
Noise power	-90dBm
Convergence precision	10^{-4}
Reference Path loss	-30dB
BS position	(0,0,10)
RIS position	(30,0,10)

Volume 17- Number 2 - 2025 (1-8)

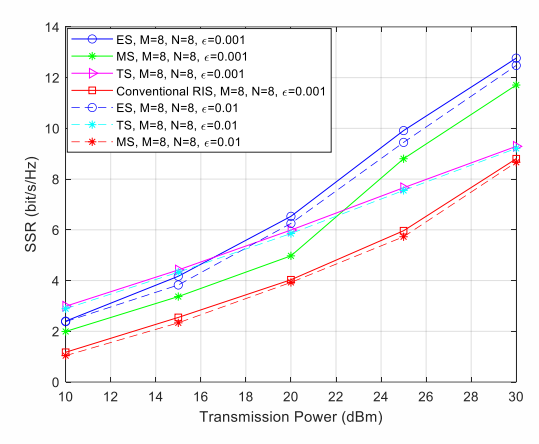


Figure 2. Sum secrecy rate versus the transmission power

Fig.3 presents the sum secrecy rate versus the number of Star-RIS elements. By increasing M, RIS can receive a greater amount of signal power, and beamforming can be done with more degrees of freedom, so the SSR improves for all methods.

Among all deployment methods, Star-RIS outperforms conventional RIS due to more DoFs. In Star-RIS deployment models, TS outperforms ES and MS due to interference-free communications. As previous figure, ES outperforms MS since MS is a special case of ES with binary amplitude coefficients. Moreover, this figure shows that ES and MS with the assumption of perfect CSI have higher performance than imperfect CSI over CSI error $\epsilon = 0.001$ due to enabling BS for more accurate beamforming.

This figure confirms the impact of optimization over the vector of passive beamforming, which means RIS transmission and reflection coefficients. It can be seen from Fig.4 over CSI error 0.001 and power budget 10dBm, that higher number of transmitting antennas leads to a rise in the overall secrecy rate of legitimate users since more BS antennas enable higher active beamforming gain and brings more DoFs, which confirms the impact of optimization over active beamforming.

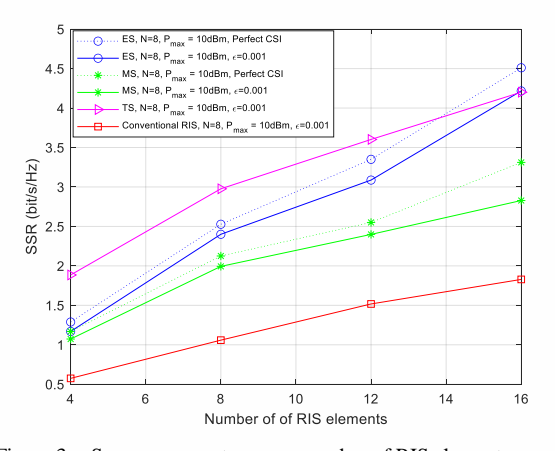


Figure 3. Sum secrecy rate versus number of RIS element.

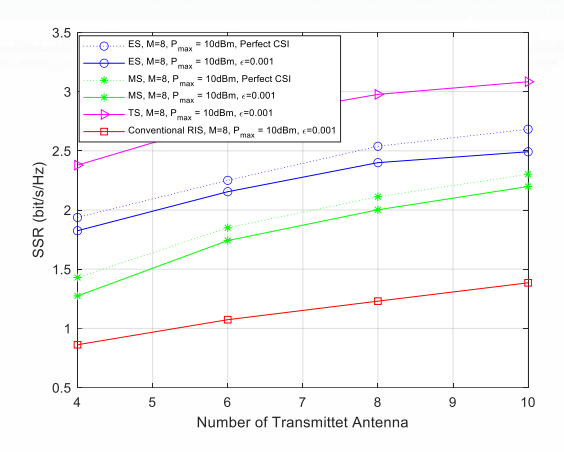


Figure 4. Sum secrecy rate versus number of BS antenna

As the previous figures, we can see that Star-RIS outperforms conventional RIS. In Star-RIS deployment model, TS outperforms ES and MS due to interference-free communications, and ES outperforms MS since MS is a special case of ES with fewer DoFs. Moreover, ES and MS with the assumption of perfect CSI have higher performance than imperfect CI due to enabling BS for more accurate beamforming.

Fig.5 shows the sum secrecy rate of legitimate users versus the distance between legitimate users and Star RIS over CSI error 0.001 and power budget 10dBm based on ES, MS, and TS operating protocols of Star-RIS and, conventional RIS. In all deployment methods, SSR decreases with increasing the distance between Star RIS and legitimate users due to an increase in pass loss. In the medium distance, RIS leads to better performance due to the ability to modify communication channels by changing the amplitude and phase shift of the radiated signal, but in far distance, the performance decreases.

VII. CONCLUSION

In this paper, our study is focused on investigating robust beamforming designs for secure communication aided by Star RIS in the presence of imperfect CSI. Our objective is to maximize the sum secrecy rate under the constraint of the limited transmission power budget and limited maximum eavesdropper rate by jointly optimizing active and passive beamforming at BS and

Star-RIS, respectively. We implement ES, MS, and TS protocols for Star-RIS and compare the performance with conventional RIS. According to our simulation findings, Star-RIS outperforms conventional RIS since it has more DoFs due to transmitting and reflecting signals simultaneously. In Star-RIS operating protocols, TS outperforms ES and MS when transmit power is relatively small.

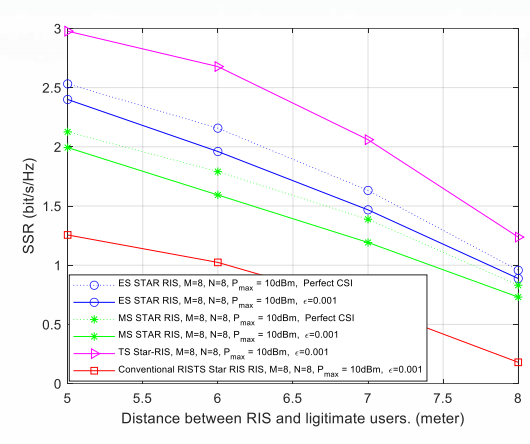


Figure 5. Sum secrecy rate versus the distance between RIS and legitimate users

Increasing the number of RIS elements and transmitter antennas leads to higher performance due to higher beamforming gain. Our results show performance degradation with higher CSI estimation error due to more difficulty in accurate beamforming.

REFERENCES

- [1] M. A. A. Junior, G. Fraidenraich, R. C. Ferreira, F. A. De Figueiredo, and E. R. De Lima, "Multiple-antenna weibull-fading wireless communications enhanced by reconfigurable intelligent surfaces," *IEEE Access*, vol. 11, pp. 107218-107236, 2023.
- [2] Q. Wu, S. Zhang, B. Zheng, C. You, and R. Zhang, "Intelligent reflecting surface-aided wireless communications: A tutorial," *IEEE transactions on communications*, vol. 69, no. 5, pp. 3313-3351, 2021.
- [3] L. Hu, C. Sun, G. Li, A. Hu, and D. W. K. Ng, "Reconfigurable Intelligent Surface-aided Secret Key Generation in Multi-Cell Systems," *IEEE Transactions on Communications*, 2023.
- [4] M. A. Parhizgar and S. M. Razavizadeh, "AN-aided beamforming for IRS-assisted SWIPT systems," *Physical Communication*, vol. 54, p. 101816, 2022.
- [5] S. Xu, C. Liu, H. Wang, M. Qian, and J. Li, "On secrecy performance analysis of multi-antenna STAR-RISassisted downlink NOMA systems," *EURASIP Journal* on Advances in Signal Processing, vol. 2022, no. 1, p. 118, 2022.
- [6] Y. Lin, Y. Shen, and A. Li, "Simultaneous transmission and reflection beamforming design for RIS-aided MU-MISO," *IEEE Transactions on Vehicular Technology*, vol. 72, no. 3, pp. 4040-4045, 2022.
- [7] X. Yu, D. Xu, Y. Sun, D. W. K. Ng, and R. Schober, "Robust and secure wireless communications via intelligent reflecting surfaces," *IEEE Journal on Selected Areas in Communications*, vol. 38, no. 11, pp. 2637-2652, 2020.
- [8] X. Mu, Y. Liu, L. Guo, J. Lin, and R. Schober, "Simultaneously transmitting and reflecting (STAR) RIS aided wireless communications," *IEEE Transactions on Wireless Communications*, vol. 21, no. 5, pp. 3083-3098, 2021.
- [9] G. Zhou, C. Pan, H. Ren, K. Wang, and A. Nallanathan, "A framework of robust transmission design for IRS-aided MISO communications with imperfect cascaded channels," *IEEE Transactions on Signal Processing*, vol. 68, pp. 5092-5106, 2020.
- [10] S. R. Shahcheragh and K. Mohamed-Pour, "Active and Passive Beamforming for Secure Wireless Communication via Star-RIS Under Imperfect CSI," in 2023 31st International Conference on Electrical Engineering (ICEE), 2023: IEEE, pp. 981-986.
- [11] H. Niu, Z. Chu, F. Zhou, and Z. Zhu, "Simultaneous transmission and reflection reconfigurable intelligent

- surface assisted secrecy MISO networks," *IEEE Communications Letters*, vol. 25, no. 11, pp. 3498-3502, 2021
- [12] B. Shi et al., "STAR-RIS-UAV-aided coordinated multipoint cellular system for multi-user networks," *Drones*, vol. 7, no. 6, p. 403, 2023.
- [13] H. Niu, Z. Chu, F. Zhou, P. Xiao, and N. Al-Dhahir, "Simultaneous transmission and reflection reconfigurable intelligent surface assisted MIMO systems," arXiv preprint arXiv:2106.09450, 2021.
- [14] J. Zuo, Y. Liu, Z. Ding, L. Song, and H. V. Poor, "Joint design for simultaneously transmitting and reflecting (STAR) RIS assisted NOMA systems," *IEEE Transactions on Wireless Communications*, vol. 22, no. 1, pp. 611-626, 2022.
- [15] Y. Sun, K. An, J. Luo, Y. Zhu, G. Zheng, and S. Chatzinotas, "Intelligent reflecting surface enhanced secure transmission against both jamming and eavesdropping attacks," *IEEE Transactions on Vehicular Technology*, vol. 70, no. 10, pp. 11017-11022, 2021.



Kamal Mohamed-pour was born in Iran in 1954, and received his B.S. and M.Sc. in Electrical Engineering in the field of communications in Tehran, 1979 and 1987 respectively.

After some lecturing in department of Communication in Electrical

engineering faculty of K.N. Toosi University of Technology, continued his study towards Ph.D., and graduated at 1996 in Elec. Eng. at University of Manchester, Manchester, UK.

Dr. Mohamed-pour is a full professor in communication department of K.N. Toosi University of Technology, and published several books in digital signal processing and communications. His main interest fields of research are wide-band Wireless communication, MIMO-OFDM, and Relay Networks.



Seyedeh Reyhane Shahcheragh was born in 1992. She received B.Sc. degree in Electrical Engineering from Iran University of Science & Technology, Tehran, Iran, in 2015 and M.Sc. degree in Electrical Engineering from Shahrood

University of Technology, in 2018, and Ph.D. degree from K. N. Toosi University of Technology in Electrical Engineering in the field of Communication Systems in 2025. She is a member of Iran's National Elites Foundation. Her research interests include Wireless Communication, Secrecy communications, and Star-RIS.